BLED WORKSHOPS
IN PHYSICS
VOL. 12, NO. 1
p. 7

Proceedings of the Mini-Workshop
Understanding hadronic spectra
Bled, Slovenia, July 3 - 10, 2011

0^{++} states in a large-N_c Regge approach*

Enrique Ruiz Arriola[a] and Wojciech Broniowski [b]

[a]Departamento de Física Atómica, Molecular y Nuclear and Instituto Carlos I de Física Teórica y Computacional, Universidad de Granada, E-18071 Granada, Spain
[b]The H. Niewodniczański Institute of Nuclear Physics PAN, PL-31342 Kraków, Poland, and Institute of Physics, Jan Kochanowski University, PL-25406 Kielce, Poland

Abstract. Scalar-isoscalar states ($J^{PC} = 0^{++}$) are discussed within the large-N_c Regge approach. We find that the lightest $f_0(600)$ scalar-isoscalar state fits very well into the pattern of the radial Regge trajectory where the resonance nature of the states is advantageously used. We confirm the obtained mass values from an analysis of the pion and nucleon spin-0 gravitational form factors, recently measured on the lattice. We provide arguments suggesting an alternating meson-glueball pattern of the 0^{++} states, which is supported by the pseudoscalar-isovector 0^{+-} excited spectrum and asymptotic chiral symmetry. Finally, matching to the OPE requires a fine-tuned mass condition of the vanishing dimension-2 condensate in the Regge approach with infinitely many scalar-isoscalar states.

1 Introduction

The goal of this talk is to discuss various intriguing aspects of the spectrum of scalar-isoscalar states. Approaches developed in recent years may shed new light on this long-elaborated problem in hadronic physics.

Subsequent hadron resonances listed in the Particle Data Group (PDG) tables increase their mass up to the upper experimental limit of 2.5 GeV, while their width remains bound within 500 MeV. In Fig. 1 we show separately the widths of all baryons and mesons listed in the PDG tables [1] as functions of the mass of the state. One naturally expects that broad resonances, i.e., with $\Gamma \sim m$, escape phenomenological analysis; even if they existed, they might be missing from the PDG as difficult to assess experimentally. Note, however, that with the exception of the notorious $f_0(600)$ resonance and a few baryon and meson states, the ratio is bound by the line $\Gamma/m \sim 1/3$ (the dashed line in Fig. 2).

A natural and model-independent framework to understand this feature is provided by the limit of large number of colors in QCD. Indeed, in this large-N_c limit, with $g^2 N_c$ fixed, baryons are heavy with mass $m = \mathcal{O}(N_c)$ and width $\Gamma = \mathcal{O}(N_c^0)$ [2,3], while mesons and glueballs are stable, with mass independent of N_c, namely $m = \mathcal{O}(N_c^0)$, and width Γ suppressed as $1/N_c$ and $1/N_c^2$, respectively. This means that Γ/m is suppressed (see, e.g., [4] for a review). In particular, one has $\Gamma/m \sim N_c^{-1}$ for mesons and baryons, while $\Gamma/m \sim N_c^{-2}$ for glueballs.[1]

* Talk delivered by Enrique Ruiz Arriola

[1] Fig. 1 suggests that it is reasonable to assume that excited states in the spectrum follow a more accurate large-N_c pattern than the ground state.

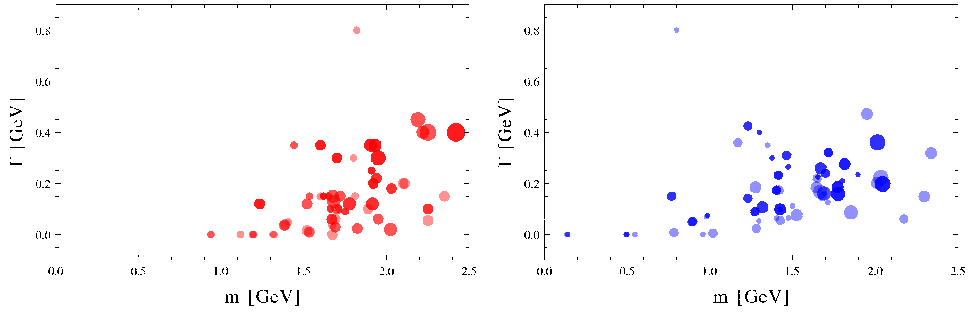

Fig. 1. Width of *all* baryons (left panel) and mesons (right panel) listed in the PDG tables [1] as a function of the hadron mass (in GeV). The surface of each point is proportional to the $(2J+1)$ spin degeneracy, while the intensity is proportional to the isospin degeneracy $(2I+1)$.

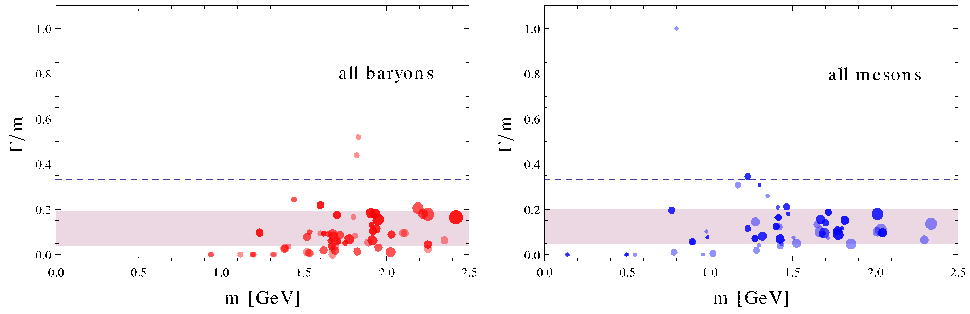

Fig. 2. Same as Fig. 1 for the width/mass ratio. The large-N_c limit predicts $\Gamma/m \sim \mathcal{O}(N_c^{-1})$. The dashed horizontal line corresponds to $1/3$. The gray bands reflect the uncertainties of the fit $\Gamma/m = 0.12(8)$.

On the other hand, at high excitations mesons are expected to resemble strings of length $l \sim m/\sigma$, with σ denoting the string tension (see, e.g., Ref. [5] and references therein). Actually, the decay rate of a string per unit time, Γ, is estimated to be proportional to the length [6,7], which immediately yields constant Γ/m.[2] In Fig. 2 we show the ratio of widths to masses of *all* baryons and mesons listed in the PDG tables [1], plotted as functions of the mass of the state. If we compute the average weighted with the $(2J+1)$ spin degeneracy and its spread, we find (α are the remaining quantum numbers, including isospin)

$$\frac{\Gamma}{m} \equiv \sum_{J,\alpha} (2J+1) \frac{\Gamma_{J,\alpha}}{m_{J,\alpha}} = 0.12(8) \tag{1}$$

for both baryons and mesons! This rather small ratio, complying to the large-N_c and string-model arguments, suggests that this is a generic feature of the hadronic spectrum rather than a lack of experimental ability to resolve too broad states. One may thus assert in this regard that the PDG spectrum is fairly complete.

[2] The argument directly carries over to baryons, treated as a quark-diquark string.

2 Masses of resonances

A resonance may be interpreted as a superposition of states with a given mass distribution, approximately spanning the $m \pm \Gamma/2$ interval. Of course, the shape of the distribution depends on the particular process where the resonance is produced, and thus on the background. The rigorous quantum-mechanical definition of the resonance corresponds to a pole in the second Riemann sheet in the partial-wave amplitude of the corresponding decay channel, which becomes independent of the background. However, although quoting the pole is highly desirable, with a few exceptions this is *not* what one typically finds in the PDG.

As a matter of fact, several definitions are used: pole in the second Riemann sheet, pole in the K-matrix, Breit-Wigner resonance, maximum in the speed plot, time delay, etc. (see, e.g., [8, 9]). Clearly, while all these definitions converge for narrow resonances, even for broad states we expect the masses to be compatible within their corresponding $m \pm \Gamma/2$ intervals. As mentioned, the values listed in the PDG for a given resonance correspond to different choices and/or processes, but mostly the results are compatible within the estimated width differences.

The lowest resonance in QCD is the 0^{++} state $f_0(600)$ or the σ—meson. It appears as a complex pole in the second Riemann sheet of the $\pi\pi$ scattering amplitude at $\sqrt{s_\sigma} = m_\sigma - i\Gamma_\sigma/2$ with $m_\sigma = 441^{+16}_{-8}$ and $\Gamma_\sigma = 544^{+18}_{-24}$ MeV [10] (see also Ref. [11]). While these are remarkably accurate, it is unclear whether these numbers can be directly used in hadronic physics. An analysis of the role played by the σ as a correlated 2π exchange in the central component to the NN force shows that the complex-pole exchange does not accurately describe this effect in the range 1 fm $< r <$ 5 fm, but prefers a value in between the pole and the Breit-Wigner approximation, $m_\sigma = 600(50)$ MeV [12]. The Breit-Wigner parameters are $(m_\sigma, \Gamma_\sigma) = (841(5), 820(20))$ MeV [13]. For the time delay method we obtain $(m_\sigma, \Gamma_\sigma) \sim (475, 630)$ MeV. As we see, the different determinations agree within the wide $m_\sigma \pm \Gamma_\sigma/2$ interval.

3 Scalar Regge spectrum

Higher 0^{++} states listed in the PDG [1] follow roughly the general pattern of increasing mass but not their width. Radial and rotational Regge trajectories were analyzed in Ref. [14]. For scalar states [15] two parallel radial trajectories could then be identified, including three states per trajectory. In a recent work [16, 17] (see also [18]) we have analyzed all the 0^{++} states which appear in the PDG tables (see Fig. 3) and found that *all* fit into a single radial Regge trajectory of the form

$$M_S(n)^2 = \frac{a}{2} n + m_\sigma^2. \tag{2}$$

The mass of the σ state can be deduced from this trajectory as the mass of the lowest state. The resonance nature of these states suggests to use the corresponding half-width as the mass uncertainty in the χ^2 fit:

$$\chi^2 = \sum_n \left(\frac{M_{f,n} - M_S(n)}{\Gamma_{f,n}/2} \right)^2 . \tag{3}$$

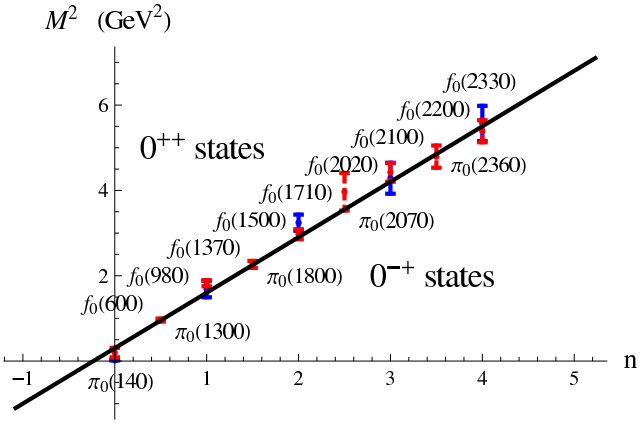

Fig. 3. Radial Regge trajectory corresponding to the squared mass of all $J^{PC} = 0^{++}$ scalar-isoscalar and $J^{PC} = 0^{-+}$ pseudoscalar-isovector states listed in the PDG tables [1]. The four heaviest 0^{++} and two 0^{-+} states are not yet well established and are omitted from the PDG summary tables. The error bars correspond to the errors in the determination of the square of mass as $\Delta m^2 = m\Gamma$ with Γ from [1]. The straight line is the result of our joined fit. Labels of 0^{++} states are above their mark whereas labels of 0^{+-} states are below their mark.

Minimization yields $\chi^2/\mathrm{DOF} = 0.12$, with

$$a = 1.31(12)\ \mathrm{GeV}^2, \qquad m_\sigma = 556(127)\ \mathrm{MeV}. \tag{4}$$

Formula (2) is actually equivalent to two parallel radial Regge trajectories with the *standard* slope,

$$M_{S,-}(n)^2 = a\,n + m_\sigma^2, \tag{5}$$

$$M_{S,+}(n)^2 = a\,n + m_\sigma^2 + \frac{a}{2}, \tag{6}$$

where $a = 2\pi\sigma$, and σ is the string tension associated to the potential $V(r) = \sigma r$ between heavy colored sources. The value $\sqrt{\sigma} = 456(21)\,\mathrm{MeV}$ obtained from our fit agrees well with lattice determinations of $\sqrt{\sigma} = 420$ MeV [19]. Of course, one expects some of these states to correspond eventually to glueballs. However, there seems to be no obvious difference between mesons and glueballs, as far as the radial Regge spectrum is concerned. Note that Casimir scaling suggests that the string tension is $\sigma_{\mathrm{glueball}} = \frac{9}{4}\sigma_{\mathrm{meson}}$, but this holds in the case of fixed and heavy sources. The fact that we have light quarks might explain why we cannot allocate easily the Casimir scaling pattern in the light-quark scalar-isoscalar spectrum.

4 Interpolating fields

For scalar states a measure of the spectrum is given in terms of the (gauge and renorm invariant) trace of the energy momentum tensor [20]

$$\Theta^\mu_\mu \equiv \Theta = \frac{\beta(\alpha)}{2\alpha} G^{\mu\nu a} G^a_{\mu\nu} + \sum_q m_q\,[1 + \gamma_m(\alpha)]\,\bar{q}q. \tag{7}$$

Here $\beta(\alpha) = \mu^2 d\alpha/d\mu^2$ denotes the beta function, $\alpha = g^2/(4\pi)$ is the running coupling constant, $\gamma_m(\alpha) = d\log m/d\log\mu^2$ is the anomalous dimension of the current quark mass m_q, and $G^a_{\mu\nu}$ is the field strength tensor of the gluon field.

It is interesting to consider the situation of massless quarks, where things become somewhat simpler. Then, we have in principle two scalar operators with smallest canonical dimensions, the gluon G^2 and the quark $\bar{q}q$. While these two operators are both scalars, they are chirally even and odd, respectively, i.e., under the $q \to \gamma_5 q$ transformation. Because the chiral symmetry is spontaneously broken, there is some mixing between G^2 and $\bar{q}q$. These operators connect scalar states to the vacuum through the matrix element

$$\langle 0|\Theta|n\rangle = m_n^2 f_n\,, \qquad \langle 0|\bar{q}q|n\rangle = m_n c_n\,. \tag{8}$$

The two-point correlators read

$$\Pi_{\Theta\Theta}(q) = i\int d^4x e^{iq\cdot x}\langle 0|T\{\Theta(x)\Theta(0)\}|0\rangle = \sum_n \frac{f_n^2 m_n^4}{m_n^2 - q^2} + \text{c.t.}\,, \tag{9}$$

$$\Pi_{\Theta S}(q) = i\int d^4x e^{iq\cdot x}\langle 0|T\{\Theta(x)\bar{q}q(0)\}|0\rangle = \sum_n \frac{f_n^2 m_n^2 c_n m_n}{m_n^2 - q^2} + \text{c.t.}\,, \tag{10}$$

$$\Pi_{SS}(q) = i\int d^4x e^{iq\cdot x}\langle 0|T\{\bar{q}q(x)\bar{q}q(0)\}|0\rangle = \sum_n \frac{c_n^2 m_n^2}{m_n^2 - q^2} + \text{c.t.}\,, \tag{11}$$

where in the r.h.s. we saturate with scalar states and c.t. stands for subtraction constants which can chosen as to replace $m_n^2 \to q^2$ in the numerator. In that scheme, in the large $-q^2 \gg \Lambda_{QCD}$ limit, a comparison with the Operator Product Expansion (OPE) [21–23] leads to the matching conditions

$$\begin{aligned}
\Pi_{\Theta\Theta}(q^2) &= q^4\, C_0\, \log(-q^2) + \ldots\,,\\
\Pi_{SS}(q^2) &= q^2\, C_0'\, \log(-q^2) + \ldots\,,\\
\Pi_{\Theta S}(q^2) &= C_0''\,\langle\bar{q}q\rangle \log(-q^2) + \ldots\,,
\end{aligned} \tag{12}$$

where $C_0 = -(2\beta(\alpha)/\alpha\pi)^2$, $C_0' = -3/(8\pi^2)$ and $C_0'' = -2\beta(\alpha)/\alpha\pi$. As we see, $\bar{q}q$ and G^2 do not mix at high q^2 values, a consequence of asymptotic chiral symmetry [20]. In these limits the sums over n can be replaced by integrals, whence the following asymptotic conditions are found:

$$f_n^2/(dm_n^2/dn) \to C_0\,, \quad c_n^2/(dm_n^2/dn) \to C_0'\,, \quad c_n f_n m_n^3/(dm_n^2/dn) \to C_0''\langle\bar{q}q\rangle \tag{13}$$

We see that the first two conditions are incompatible with the third one if m_n increases for large n, as is the case of the data. However, if we group the states in two families, as suggested by Eqs. (6) and Fig. 3, we get a compatible solution

$$c_{n,-}, f_{n,+} \to \text{const} \qquad c_{n,+}, f_{n,-} \to \text{const}/m_n^3. \tag{14}$$

This is equivalent to assuming an asymptotically alternating pattern of mesons and glueballs, coupling to chirally odd and even operators, $\bar{q}q$ and G^2, respectively. Since asymptotically $m_n^2 \sim an/2$, we find $c_{n,-}/c_{n,+}$ and $f_{n,+}/f_{n,-} \sim n^{\frac{3}{2}}$. Of course, this is not the only solution.

The situation described above suggests the existence of a hidden symmetry in the 0^{++} sector. In our case we could think of the γ_5-parity (which becomes a good quantum number for excited states) as the relevant symmetry which makes the difference between the chirally even and odd states. This, however, only explains the fact that asymptotically the slopes of the $+$ and $-$ branches are the same, but not why the intercepts accurately differ by half the slope.

5 The holographic connection

To further elaborate on this intriguing point of the accidental degeneracy, let us consider the one-dimensional harmonic oscillator with frequency ω, as an example; all states $\psi_n(z)$ with the energy $E_n = \hbar\omega(n + 1/2)$ can be separated into parity *even* and parity *odd* states, satisfying the conditions $\psi_{n,\pm}(z) = \psi_{2n}(z)$ and $\psi_{\pm,n}(-z) = \pm\psi_{\pm,n}(z)$, respectively, and having the energies $E_{+,n} = 2\hbar\omega(n+1/4)$ and $E_{-,n} = 2\hbar\omega(n + 3/4)$. These formulas display *twice* the slope of E_n. Thus, given the states with energies $E_{+,n}$ and $E_{-,n}$, we might infer that parity was a hidden symmetry of a Hamiltonian explaining the correlation between the slope and intercepts.

In the relativistic case the argument can also be made in a suggestive manner. Let us consider the Klein-Gordon action for infinitely many bosons in four dimensions, described with fields $\phi_n(x)$ of masses m_n:

$$S = \frac{1}{2}\int d^4x \sum_n \left[\partial^\mu\phi_n\partial_\mu\phi_n - m_n^2\phi_n^2\right]. \tag{15}$$

We assume the spectrum of the form $m_n^2 = an + m_0^2$. Next, we can introduce the five-dimensional field $\phi(x,z) = \sum_n \phi_n(x)\psi_n(z)$, with $\psi_n(z)$ fulfilling the auxiliary Sturm-Liouville problem in the variable $0 \le z < \infty$,

$$-\partial_z\left[p(z)\partial_z\psi_n(z)\right] + q(z)\psi_n(z) = m_n^2\rho(z)\psi_n(z), \tag{16}$$

where the functions are orthogonal with respect to the weight function $\rho(z)$, provided suitable boundary conditions

$$p(z)\left(\psi_n'(z)\psi_m(z) - \psi_n(z)\psi_m'(z)\right)|_{z=0} = 0 \tag{17}$$

and $\psi_n(\infty) \to 0$ are fulfilled. The action can then be written as

$$S = \frac{1}{2}\int d^4x \int_0^\infty dz\left[\rho(z)\partial^\mu\phi\partial_\mu\phi - p(z)(\partial_z\phi)^2 - q(z)\phi^2\right] \tag{18}$$

after some integration by parts in the variable z. This action can be written as a five-dimensional action with a non-trivial metric [24], featuring the AdS/CFT (soft-wall) approach (see [25] and references therein), with the extra dimension z playing the role of a holographic variable and the orthogonal set of functions $\psi_n(z)$ denoting the corresponding Kaluza-Klein modes. Clearly, z has the dimension of length, suggesting that $z \to 0$ corresponds to the ultraviolet and $z \to \infty$ to the infrared regime.

Turning to Eq. (16), we may take the standard Harmonic oscillator Schrödinger-like equation ($p(z) = \rho(z) = 1$, $q(z) \equiv U(z) = a^2 z^2/16$)

$$-\psi_n''(z) + \frac{1}{16} a^2 z^2 \psi_n(z) = m_n^2 \psi_n(z) \tag{19}$$

and obtain for the regular solutions at infinity the result

$$\frac{\psi_n'(0)}{\psi_n(0)} = -\sqrt{a}\, \frac{\Gamma\left(\frac{3}{4} - \frac{m_n^2}{a}\right)}{\Gamma\left(\frac{1}{4} - \frac{m_n^2}{a}\right)}, \tag{20}$$

where $\Gamma(x)$ is the Euler Gamma function, which is meromorphic and have simple poles at $x = 0, -1, -2, \ldots$. The solutions fulfilling the Dirichlet, $\psi_n(0) = 0$, and Neumann, $\psi_n'(0) = 0$, boundary conditions, respectively, have the masses

$$m_{-,n}^2 = an + \frac{a}{4}\,, \qquad m_{+,n}^2 = an + \frac{3a}{4}\,, \tag{21}$$

which can be merged into one single formula

$$m_n^2 = \frac{a}{4}(2n + 1)\,. \tag{22}$$

This yields $m_\sigma = m_{f_0}/\sqrt{3} = 566$ MeV and, for the string tension, $\sigma = m_{f_0}\sqrt{2/3\pi} = 450$ MeV with $m_{f_0} = 980$ MeV, quite reasonable values.

In this approach the symmetry in the scalar spectrum corresponds to a parity symmetry in the holographic z variable $\psi_n(-z) = \pm\psi_n(z)$. Note that usually the holographic variable z is taken to be positive[3], but if we extend it to $-\infty < z < \infty$, we may define a holographic superfield containing two different and orthogonal modes. Otherwise, in the interval $0 < z < \infty$ the Dirichlet and Neumann modes are not orthogonal to each other.

6 Pseudoscalar mesons and chiral symmetry

Discerning the nature of the σ state has been a recurrent pastime for many years. As is well known, glueballs are more weakly coupled to mesons, $\mathcal{O}(1/N_C)$, than other mesons, $\mathcal{O}(1/\sqrt{N_C})$. The minimum number of states, allowed by certain sum rules and low energy theorems, is just two. In Ref. [16] we undertake such an analysis which suggests that $f_0(600)$ (denoted as σ) is a $\bar{q}q$ meson, while $f_0(980)$ (denoted as f_0) is a glueball. This is supported by the rather small width ratio,

[3] This is supported by the light-front interpretation of Brodsky and de Teramond [26], where the holographic variable is the polar coordinate of a two dimensional vector, $z = |\zeta|$ and $\zeta = b\sqrt{x(1-x)}$, with b denoting the impact parameter and x the momentum fraction of the quark. This interpretation yields a two dimensional potential $U(\zeta) = \kappa^2\zeta^2 + 2\kappa^2(L + S - 1)$ with $J = L + S$ which, when passing to the polar variable z, generates the usual centrifugal term $(L^2 - 1/4)/z^2$ not present in our discussion, yielding $M_{n,L,S}^2 = 4\kappa^2(n + L + S/2)$ which for $J = 0$ and $L = 1$ resembles Eq. (22).

which yields $\Gamma_f/\Gamma_\sigma \sim (g^2_{f\pi\pi} m_f^3)/(g^2_{\sigma\pi\pi} m_\sigma^3) \sim 1/N_C$, thus for $m_\sigma \sim 0.8$ MeV $\sim m_f$ the ratio $g_{\sigma\pi\pi}/g_{f\pi\pi} \sim \sqrt{N_C}$ is obtained.

A further piece of evidence for the alternating meson-glueball pattern is provided by looking at the excited pion spectrum, which we show in Fig. 3. The alternating pattern was unveiled by Glozman [27], suggesting that states degenerate with the pion might not be identified with glueballs. Remarkably, the states generating doublets with pion states are $f_0(600) \leftrightarrow \pi_0(140)$, $f_0(1370) \leftrightarrow \pi_0(1300)$, $f_0(1710) \leftrightarrow \pi_0(1800)$, $f_0(2100) \leftrightarrow \pi_0(2070)$, and $f_0(2330) \leftrightarrow \pi_0(2360)$, whereas the other scalar states $f_0(980)$, $f_0(1500)$, $f_0(2020)$ and $f_0(2200)$ are not degenerate with other mesons with light u and d quarks. Our analysis is reinforced by this observation.

As a matter of fact, fitting the pion $\pi(140)$ as the $n = 0$ state of the Regge spectrum requires strong departure from a simple linear trajectory, $m_n^2 = an + m_0^2$. One may improve on this by using the holographic connection and a mixed boundary condition at $z = 0$ determined by fixing the mass of the ground state m_0 using Eq. (17) together with Eq. (20) for the harmonic oscillator case, Eq. (19). This procedure ensures the orthogonality between all states and implements linearity for large n. This can be done for the ground states $m_0 = m_\pi, m_\sigma, m_{f_0}$. The fit to all states yields $a = 1.37\text{GeV}^2$ and the mass spectra (in GeV)

π (Regge) $(0.140, 1.260, 1.730, 2.092, 2.400, \dots)$ π (PDG) $(0.140, 1.300, 1.812, 2.070, 2.360)$
σ (Regge) $(0.527, 1.297, 1.750, 2.106, 2.411, \dots)$ σ (PDG) $(0.600, 1.350, 1.724, 2.103, 2.321)$
f_0 (Regge) $(0.977, 1.513, 1.906, 2.232, 2.517, \dots)$ f_0 (PDG) $(0.980, 1.505, 1.992, 2.189)$

yielding $1/\sqrt{a}\,\psi_0'(0)/\psi_0(0) = -3.1$, -14.9, and 0.2, respectively. Note the large and small values for the σ and f_0 cases, which suggests that these boundary conditions are very close to the Dirichlet and Neumann cases. Chiral symmetry breaking corresponds to the different π and σ values.

7 Scalar dominance and heavy pions

Hadronic matrix elements of the energy-momentum tensor, the so-called gravitational form factors (GFF) of the pion and nucleon, correspond to a dominance of scalar states in the large-N_c picture, as ($u(p)$ is a Dirac spinor)

$$\langle \pi(p')|\Theta|\pi(p)\rangle = \sum_n \frac{g_{n\pi\pi} f_n q^2 m_n^2}{m_n^2 - q^2}, \tag{23}$$

$$\langle N(p')|\Theta|N(p)\rangle = \bar{u}(p')u(p) \sum_n \frac{g_{nNN} f_n m_n^2}{m_n^2 - q^2}, \tag{24}$$

where the sum rules $\sum_n g_{n\pi\pi} f_n = 1$ [28] and $M_N = \sum_n g_{nNN} f_n$ [29] hold. Unfortunately, the lattice QCD data for the pion [30] and nucleon (LHPC [31] and QCDSF [32] collaborations), picking the valence quark contribution, are too noisy as to pin down the coupling of the excited scalar-isoscalar states to the energy-momentum tensor. Nevertheless, useful information confirming the (Regge) mass estimates for the σ-meson can be extracted [16] through the use of the multiplicative QCD evolution of the GFF in the valence quark momentum fraction, $\langle x\rangle_{u+d}$,

m_π[MeV]	m_σ [MeV]	m_σ [MeV]	m_σ [MeV]	m_σ [MeV]
	GFF	GFF	$(\bar{q}q)^2$-dynam.	$(\bar{q}q)^2$-quench.
230	580(190)	620(100)	–	400(30)
342	630(190)	660(90)	–	720(20)
478	710(200)	730(90)	–	1000(20)
318	620(190)	650(90)	468(50)	–
469	700(190)	720(90)	936(13)	–
526	739(200)	750(90)	1066(13)	–

Table 1. Scalar monopole mass obtained from the nucleon gravitational form factors, extracted from the $(\bar{q}q)$ components obtained by LHPC [31] and QCDSF [32] and compared to the lattice calculation using the tetraquark $(\bar{q}q)^2$ probing fields, both for the dynamical and quenched fermions [33] .

as seen in deep inelastic scattering or on the lattice at the scale $\mu = 2$ GeV. For the pion and nucleon GFFs we obtain the fits

$$\langle x\rangle^{\pi}_{u+d} = 0.52(2), \qquad m_\sigma = 445(32)\ \text{MeV}\,, \tag{25}$$
$$\langle x\rangle^{N}_{u+d} = 0.447(14), \qquad m_\sigma = 550^{+180}_{-200}\text{MeV}. \tag{26}$$

Assuming a simple dependence of m_σ on m_π,

$$m_\sigma^2(m_\pi) = m_\sigma^2 + c\left(m_\pi^2 - m_{\pi,\text{phys}}^2\right), \tag{27}$$

yields $m_\sigma = 550^{+180}_{-200}$MeV and $c = 0.95^{+0.80}_{-0.75}$, or $m_\sigma = 600^{+80}_{-100}$MeV and $c = 0.8(2)$, depending on the choice of the lattice data [31] or [32], respectively. Note that c is close to unity. *Higher* quark masses might possibly clarify whether or not the state evolves into a glueball or a meson. For a $(\bar{q}q)^n$ system one expects $m_\sigma \to 2n m_q + \text{const}$ at large current quark mass m_q. The data from [31] or [32] are too noisy to see the difference, although for the largest pion masses we see that $m_\sigma \sim m_\pi$, as it simply corresponds to the $\bar{q}q$-component of Θ. We observe, however, that for $m_\pi \sim 500$MeV our results are not far away from the recent lattice calculation using the tetraquark probes, $(\bar{q}q)^2$ [33], which provide $m_\sigma \sim 2m_\pi$ for the largest pion masses as they should (see Table 1). From this viewpoint, and unless operator mixing is implemented, the nature of the state is predetermined by the probing operator.

8 Dimension-2 condensates

One of the problems of the large-N_c Regge models [35] and their holographic relatives [36, 37] is that they may contradict expectations from the OPE, as they involve dimension-2 condensates. For instance, the OPE for the $\Pi_{\Theta\Theta}(q^2)$ correlator in Eq.(12) gives corrections $\mathcal{O}(q^0)$, while the $\mathcal{O}(q^2)$ terms are missing [21].

This yields a one to one comparison:

$$C_0 = -\lim_{n\to\infty} \frac{f_n^2}{dm_n^2/dn} = -\frac{N_c^2-1}{2\pi^2}\left(\frac{\beta(\alpha)}{\alpha}\right)^2, \tag{28}$$

$$C_2 = \sum_n f_n^2 = 0\,, \tag{29}$$

$$C_4 = \sum_n f_n^2 m_n^2 = \left(\frac{\beta(\alpha)}{\alpha}\right)^2 \langle G^2\rangle\,. \tag{30}$$

Equation (28) requires infinitely many states, while Eq. (29) suggests a positive and non-vanishing gauge-invariant dimension-2 object, $C_2 = i\int d^4x x^2\langle\Theta(x)\Theta\rangle$, which is generally non-local, as it should not appear in the OPE. Note that $C_2 > 0$, hence is non-vanishing for a finite number of states. The infinite Regge spectrum of Eq. (2) with Eq. (28) may be modeled with a constant $f_{f_0} = f_{n,+} = \mathcal{O}(N_c)$ whereas $f_{n,-} = \mathcal{O}(\sqrt{N_c})$ goes as Eq. (14) and yields a convergent and hence positive contribution. Naively, we get $C_2 = \infty$. However, C_2 may vanish, as required by standard OPE, when infinitely many states are considered *after regularization*. The use of the ζ-function regularization [16,34] gives

$$C_2 \equiv \lim_{s\to 0}\sum f_n^2 M_S(n)^{2s} = \sum_n f_{n,-}^2 + f_{f_0}^2\left(1/2 - m_{f_0}^2/a\right)\,. \tag{31}$$

Then $C_2 = 0$ for $m_{f_0} > \sqrt{a/2} = 810(40)$ MeV, a reasonable value to $\mathcal{O}(1/N_c)$ In any case, the important remark is that while at the OPE level $C_2 = 0$ vanishes for trivial reasons, at the Regge spectrum level some fine tuning must be at work.

Acknowledgments This work is partially supported by the Polish Ministry of Science and Higher Education (grants N N202 263438 and N N202 249235), Spanish DGI and FEDER funds (grant FIS2008-01143/FIS), Junta de Andalucía (grant FQM225-05).

References

1. C. Amsler, et al., *Phys. Lett.* **B667**, 1 (2008).
2. E. Witten, Nucl. Phys. **B160**, 57 (1979).
3. W. Broniowski, Nucl. Phys. **A580**, 429 (1994), hep-ph/9402206.
4. A. Pich (2002), hep-ph/0205030.
5. A. Andrianov, D. Espriu, and A. Prats, *Int.J.Mod.Phys.* **A21**, 3337 (2006), hep-th/0507212.
6. E. Gurvich, *Phys.Lett.* **B87**, 386 (1979).
7. A. Casher, H. Neuberger, and S. Nussinov, *Phys.Rev.* **D20**, 179 (1979).
8. N. Suzuki, T. Sato, and T.-S. Lee, *Phys.Rev.* **C79**, 025205 (2009), 0806.2043.
9. R. Workman, R. Arndt, and M. Paris, *Phys.Rev.* **C79**, 038201 (2009), 0808.2176.
10. I. Caprini, G. Colangelo, and H. Leutwyler, *Phys. Rev. Lett.* **96**, 132001 (2006), hep-ph/0512364.
11. R. Garcia-Martin, R. Kaminski, J. R. Pelaez, and J. Ruiz de Elvira, *Phys. Rev. Lett.* **107**, 072001 (2011), 1107.1635.

12. A. Calle Cordon, and E. Ruiz Arriola, *Phys. Rev.* **C80**, 014002 (2009), nucl-th/0904.0421.
13. J. Nieves, A. Pich, and E. Ruiz Arriola *Phys. Rev.* **D** (2011) (in press), hep-ph/1107.3247.
14. A. V. Anisovich, V. V. Anisovich, and A. V. Sarantsev, *Phys. Rev.* **D62**, 051502 (2000), hep-ph/0003113.
15. V. V. Anisovich, *Int. J. Mod. Phys.* **A21**, 3615 (2006), hep-ph/0510409.
16. E. Ruiz Arriola, and W. Broniowski, *Phys. Rev.* **D81**, 054009 (2010), 1001.1636.
17. E. R. Arriola, W. Broniowski, AIP Conf. Proc. **1343**, 361 (2011), 1011.5176.
18. W. de Paula, and T. Frederico, *Phys.Lett.* **B693**, 287 (2010), 0908.4282.
19. O. Kaczmarek, and F. Zantow, *Phys. Rev.* **D71**, 114510 (2005), hep-lat/0503017.
20. J. F. Donoghue, and H. Leutwyler, *Z. Phys.* **C52**, 343 (1991).
21. S. Narison, *Nucl. Phys.* **B509**, 312 (1998), hep-ph/9612457.
22. S. Narison, N. Pak, N. Paver, Phys. Lett. **B147** (1984) 162.
23. D. Harnett, R. T. Kleiv, K. Moats, T. G. Steele, Nucl. Phys. **A850**, 110-135 (2011).
24. S. S. Afonin, Int. J. Mod. Phys. **A25**, 5683 (2010), 1001.3105.
25. J. Erdmenger, N. Evans, I. Kirsch, E. Threlfall, Eur. Phys. J. **A35**, 81 (2008), 0711.4467.
26. G. F. de Teramond, S. J. Brodsky, Phys. Rev. Lett. **102** (2009) 081601. [arXiv:0809.4899 [hep-ph]].
27. L. Glozman, *Eur.Phys.J.* **A19**, 153 (2004), hep-ph/0301012.
28. S. Narison, and G. Veneziano, *Int. J. Mod. Phys.* **A4**, 2751 (1989).
29. P. Carruthers, *Phys. Rept.* **1**, 1 (1971).
30. D. Brommel, et al. (2007), 0708.2249.
31. P. Hagler, et al., *Phys. Rev.* **D77**, 094502 (2008), 0705.4295.
32. M. Gockeler, et al., *Phys. Rev. Lett.* **92**, 042002 (2004), hep-ph/0304249.
33. S. Prelovsek, T. Draper, C. B. Lang, M. Limmer, K.-F. Liu, et al., *Phys.Rev.* **D82**, 094507 (2010), 1005.0948.
34. E. R. Arriola, and W. Broniowski, *Eur. Phys. J.* **A31**, 739–741 (2007), hep-ph/0609266.
35. E. Ruiz Arriola, W. Broniowski, Phys. Rev. **D73** (2006) 097502.
36. O. Andreev, Phys. Rev. **D73** (2006) 107901.
37. F. Zuo, T. Huang, [arXiv:0801.1172 [hep-ph]].